Macromolecules

ARTICLE

pubs.acs.org/Macromolecules

What Determines the Lamellar Orientation on Substrates?

Ju-Ping Yang,[†] Qi Liao,[*,†] Jian-Jun Zhou,[‡] Xi Jiang,[†] Xiao-Hong Wang,[†] Yang Zhang,[†] Shi-Dong Jiang,[§] Shou-Ke Yan,[§] and Lin Li[*,†,‡]

[†]Laboratory of Polymer Physics and Chemistry, Center for Molecular Science, Institute of Chemistry, Chinese Academy of Sciences, Beijing 100190, P. R. China

[‡]College of Chemistry, Beijing Normal University, Beijing 100875, P. R. China

[§]State Key Laboratory of Chemical Resource Engineering, Beijing University of Chemical Technology, Beijing 100029, P. R. China

Supporting Information

ABSTRACT: The recrystallization behavior of poly(ethylene oxide) (PEO) on four amorphous films of poly(vinyl alcohol) (PVA), lysozyme (LYSO), poly(vinylpyrrolidone) (PVPY), and poly(acrylic acid) (PAA) was investigated using atomic force microscopy (AFM) and transmission electron microscopy (TEM). The results show that both the degree of supercooling and PEO/substrate interactions have pronounced influence over the growth behavior of the PEO crystals. A thermodynamic model has been proposed accordingly, in which the lamellar orientation is associated with the favorite primary nucleation. We predict the lamellar orientation based on the degree of supercooling and the surface free energy of substrate. The transition of lamellar orientation from edge-on to flat-on is determined by a critical surface free energy of the substrate which is equal to the surface tension of the polymer melt.

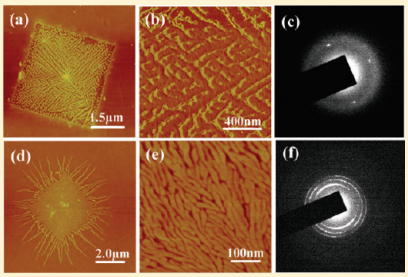

INTRODUCTION

Polymer thin films have been receiving extensive attention owing to the important role in a variety of technological applications, such as adhesion, electronics, liquid crystal alignment, and coatings.[1−3] When polymer crystallizes in thin film, the orientation of lamellae is very crucial to the film properties. Generally, there are two predominant lamellar orientations (i.e., flat-on and edge-on). In flat-on orientation, the *c*-axis of lamellae is normal to the substrate, while in edge-on orientation the *c*-axis of lamellae is parallel to the substrate. However, for polymer crystals in thin films, only one of the lamellar orientations is preferential because the lamellae cannot rotate freely during crystallization in the confined space.

It is known that the orientation of lamellae in polymer thin films is influenced by many factors, such as film thickness, crystallization temperature, and polymer/substrate interaction.[4−18] In a confined thin film system, the lamellar orientation depends on the size of confined geometry significantly, including the film thickness and the phase domain size. It has been reported that flat-on orientation is favored with the decrease of the geometry size.[4,5] The lamellar orientation could also be controlled by crystallization temperature. Many studies have shown that the transition of lamellar orientation from edge-on to flat-on generally occurs with the crystallization temperature increasing.[4,6−8] The three-layer model suggests that low temperature favors edge-on lamellae development because homogeneous nucleation forms easily at the polymer/air interface, while high temperature favors flat-on lamellae development because heterogeneous nucleation predominates at the polymer/substrate interface.[8] Another control factor may be the interaction between polymer and substrate.[9] On the basis of Monte Carlo simulations, Ma and co-workers[9] reported that for slippery substrate (repulsive interaction between polymer and substrate) edge-on lamellae develop predominantly in thin films at high temperature, while as for sticky substrate (adhesive interaction between polymer and substrate), flat-on lamellae are dominant at small film thickness. They ascribed that to the substrate-assisted crystal nucleation and the strongly inhibition of edge-on crystal thickening at the lateral growth front, respectively. However, there are also some inconsistent or interesting experimental results that predominant edge-on lamellae of PEO developed at various film thicknesses from 12 to 2500 nm and twisted lamellae of poly(L-lactide acid) from edge-on to flat-on developed during crystallization in thin films (∼100 nm).[13,19] The influence of film thickness, crystallization temperature, and the polymer/substrate interfacial interaction in particular on the lamellar orientation is still lacking coincident and comprehensive insight. It is mainly due to the difficulty to split the substrate effect from the film thickness effect and to prepare a series of flat substrates with different properties.[20]

In the present work, the melt of PEO single crystals with definite thickness about 10 nm was used to study its recrystallization behavior on solid substrates. The films of PVA, LYSO, PVPY, and PAA were chosen as substrates to study PEO/substrate interaction. Lamellar orientation of recrystallized PEO on these substrates was characterized in detail using AFM and TEM. To further explain the phenomenon, a thermodynamics model of lamellar orientation was proposed based on the structure of the primary nucleus. In particular, we focus on the dependence of the lamellar orientation upon the interfacial

Received: December 31, 2010
Revised: February 28, 2011
Published: April 14, 2011

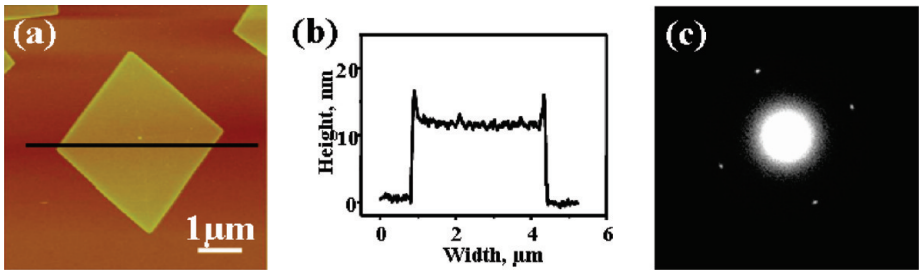

Figure 1. (a) AFM height image of a PEO single crystal, (b) the corresponding cross-section analysis, and (c) the corresponding electron diffraction pattern of a PEO single crystal.

interaction as well as the effect of the temperature on the crystallization structure.

EXPERIMENTAL SECTION

PEO (M_W = 1.0 × 10^5 g mol^{-1}), PVA (M_W = 8.5 × 10^4 g mol^{-1}), PVPY (M_W = 5.8 × 10^4 g mol^{-1}), LYSO (14.3 kDa), and PAA (M_W = 4.6 × 10^4 g mol^{-1}) were purchased from Sigma-Aldrich Chemicals and used as received. The polydispersity and melting point of PEO are 1.4 and 67 °C, respectively. Toluene was used as solvent after distillation. Silicon wafers were immersed in 30/70 (v/v) H_2O_2/H_2SO_4 for 30 min at 120 °C and then rinsed with abundant high-purity deionized water.

PEO single crystals were prepared by the self-seeding method from a 0.01 wt % toluene solution.[21] The PVA, LYSO, PVPY, and PAA films were used as substrates which were prepared by spin-coating their 1 wt % solution onto cleaned silicon wafers. Thickness and surface mean roughness of the polymer films were measured by atomic force microscopy (AFM) (Nanoscope IIIa MultiMode, Digital Instruments). The suspension containing PEO single crystals was deposited onto the substrates, and then the solvent was evaporated in a vacuum oven at 22 °C for 24 h.

PEO single crystals on different substrates were heated to 75 °C quickly and annealed for 2 min, then quenched at a rate of 130 °C/min to a selected crystallization temperature (T_c), and isothermally recrystallized for 4 h using a hot stage (FTIR600, Linkam). The height and phase images of recrystallized PEO films were acquired using tapping-mode AFM. Silicon tips (TESP) with a resonance frequency of ~300 kHz and a spring constant of about 40 N m^{-1} were used. The diffusion behavior of PEO melt on PVA, LYSO, PVPY, and PAA substrates was observed in situ using the same AFM equipped with a hot stage (Digital Instruments).

Electron diffraction (ED) was performed using a JEM-2100 TEM at an accelerating voltage of 100 kV. For PEO single crystal samples, the suspension containing PEO single crystals was directly deposited on carbon-supported TEM copper grids and then dried in a vacuum oven for 24 h at 22 °C. For PEO samples on PVPY substrate, the preparation procedures are as follows: first, the ultrathin polystyrene films were prepared on carbon-coated mica, and then the PVPY substrates were spin-coated on the surface of polystyrene films. After that, the suspension containing PEO single crystals was deposited on the prepared PVPY substrates as before. After recrystallization, the multilayered samples were floated off onto the surface of distilled water carefully and then mounted on 400 mesh electron microscopy copper grids and dried in a vacuum oven for 24 h at 22 °C. All the samples for ED experiments were prepared at the same condition as that for AFM observation.

RESULTS

PEO single crystals with regular square shape and flat surface are shown in Figure 1a. Thickness of the crystal is about 11.0 nm as shown in the cross-section analysis (Figure 1b). Figure 1c is a selective area electron diffraction pattern corresponding to the PEO single crystal. The two pairs of diffraction spots are attributed to the (120) planes of the PEO crystals with monoclinic crystal lattice.[22,23] The pattern implies that the chain-folded surface is parallel to the substrate surface (i.e., the PEO chain is perpendicular to the substrate surface). Because of the well-defined shape and uniform thickness, PEO single crystals can be taken as a perfect model system for studying polymer recrystallization behavior on substrates.

Each of PVA, LYSO, PVPY, and PAA substrates has uniform thickness and smooth surface. The thicknesses of substrates are 51, 20, 59, and 72 nm for the PVA, LYSO PVPY, and PAA, respectively, and the mean roughness of all the films is lower than 0.3 nm (see Supporting Information Table S1). Then the recrystallization behavior of PEO melts on these substrates only depends on the crystallization temperature and the interaction between PEO and substrates, while the geometrical structure of the substrates is irrelevant.

In-situ observation on the diffusion of the PEO melts on PVA, LYSO and PVPY substrates at 75 °C is shown in Figure 2. The dashed lines represent the original outlines of the PEO single crystals before melting (Figure 2a,d,g). The solid lines give the sizes of the PEO melts after annealing at 75 °C for about 2 h (Figure 2c,f,i). On PVA substrate, PEO melt shrinked significantly to its center after annealing at 75 °C for 43 min (Figure 2b). PEO melt changed to ellipsoid shape with the thickness up to about 85 nm (Figure S1) for 115 min (Figure 2c). On LYSO substrate, the size and shape of PEO melt were almost the same as that of the PEO single crystal after annealing at 75 °C for 41 and 112 min (Figure 2d–f). The height of PEO melt was also similar to that of the PEO single crystal from the AFM cross-section analyses (Figure S2). However, on PVPY substrate, the diffusion of PEO melt was clearly observed (Figure 2g–i). The size of PEO melt (solid line in Figure 2i) was obviously larger than that of the original PEO single crystal (dashed line in Figure 2g,i) after annealing at 75 °C for 110 min. At the same time, the height of PEO melt gradually decreased from the crystal center (~11 nm) to the edge (~5 nm) (Figure S3). On PAA substrate, the similar diffusion behavior as on PVPY substrate was observed. The height of PEO melt on PAA substrate decreased from the original 11 nm to about 8 nm for only 10 min incubation at 75 °C (Figure S4). The results clearly indicate that wetting of the PEO melt took place on LYSO, PVPY, and PAA substrates, while dewetting of the PEO melt occurred on PVA substrate.

The wetting or dewetting behavior of a polymer melt on a polymer substrate is related to the spreading coefficient, S, given by[24,25]

$$S = \sigma_b - (\sigma_{ab} + \sigma_a) \quad (1)$$

where σ_b and σ_a are the surface energies of an amorphous polymer substrate and PEO melt, while the σ_{ab} is the interfacial energy of the two contacting surfaces. If S is positive, the polymer melt will spread on the solid substrate; otherwise it

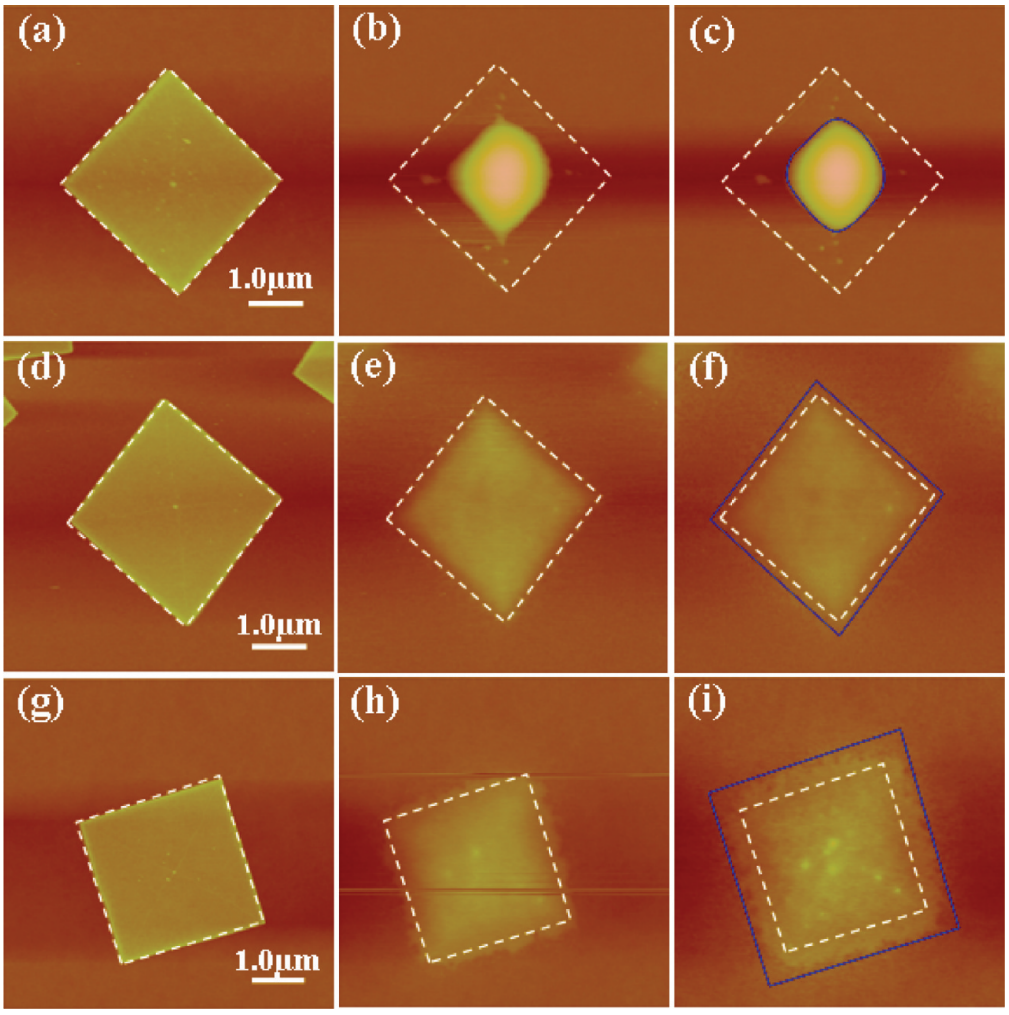

Figure 2. AFM height images show the in-situ diffusion behavior of PEO melts on different substrates: (a) the original crystal on PVA substrate at 20 °C, (b) at 75 °C for 43 min, (c) at 75 °C for 115 min; (d) the original crystal on LYSO substrate at 20 °C, (e) at 75 °C for 41 min, (f) at 75 °C for 112 min; (g) the original crystal on PVPY substrate at 20 °C, (h) at 75 °C for 40 min, (i) at 75 °C for 110 min. The dashed lines represent the original crystal outline on the three substrates, and the solid ones represent the outline after annealing at 75 °C for a certain time.

will dewet. Therefore, for PAA and PVPY substrates, $S > 0$. For LYSO substrate $S \sim 0$, and for PVA substrate $S < 0$.

Lamellar orientation of the recrystallized PEO on PVA, LYSO, and PVPY substrates obtained at different isothermal crystallization temperatures was determined using AFM and TEM ED pattern. Because of the rapid heating and cooling rate when PEO melted and recrystallized, the thickness of the PEO melts on these substrates remains almost unchanged. The diffusion of the PEO melts on LYSO, PVPY, and PAA substrates is neglectable.

The recrystallization behavior of PEO melts on different substrates was studied in detail. The results of lamellar orientation of PEO on PVPY substrate are shown in Figure 3, and the other results can be found in the supplements. When PEO melt was isothermally crystallized at a temperature above 0 °C on PVPY substrate, dendritic crystals with flat-on lamellar orientation always formed (Figure 3a,b). The ED pattern displays the diffraction of two pairs of (120) planes, which means that *c*-axis of the lamellae is normal to the substrate (Figure 3c). However, when PEO melt crystallized isothermally at a temperature below −15 °C, crystals with edge-on lamellar orientation can be observed (Figure 3d,e). Figure 3f shows the ED pattern of the crystals obtained at −15 °C. The inner ring is indexed as (120), while the outer rings consist of overlapped ($\bar{1}32$), ($0\bar{3}2$), ($\bar{2}12$) ($1\bar{1}2$), (124), (204), and (004) diffractions. Therefore, the chain direction in the crystal is parallel to substrate surface, and the crystals are not perfectly oriented edge-on lamellae.[26] Obviously, the transition of lamellar orientation from flat-on to edge-on occurs at a crystallization temperature ranging from 0 to −15 °C on PVPY substrate. The similar transition from flat-on to edge-on can be observed on PVA and LYSO substrates. The transition temperatures range from 45 to 30 °C and from 30 to 15 °C on PVA and LYSO substrates, respectively. The results are summarized in Table 1, and AFM images can be seen in the Supporting Information (Figure S5). Moreover, on PAA substrate, PEO melt cannot recrystallize in the temperature range from 45 to −30 °C due to the complex formation between PEO and PAA chains through very strong interfacial interaction.[27,28]

DISCUSSION

On the basis of our experimental results, we can conclude that for thin films with definite thickness (~10 nm) lamellar orientation is mainly controlled by two factors: the crystallization

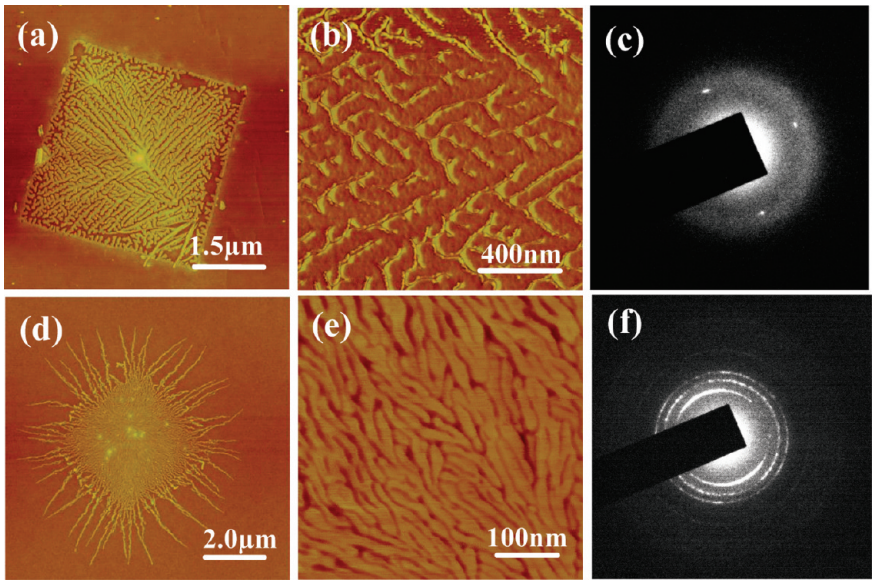

Figure 3. AFM height images show the morphologies of recrystallized PEO on PVPY film. PEO single crystals on PVPY substrate were quickly heated to 75 °C and annealed for 2 min and then quenched at a rate of 130 °C/min to a selected crystallization temperature: (a) 0 °C and (d) −15 °C. (b) and (e) are the corresponding high-resolution AFM phase images of (a) and (d). (c) and (f) are the corresponding TEM ED patterns of the PEO crystals with the same conditions as (a) and (d).

Table 1. Lamellar Orientation of PEO Crystals on PVA, PVPY, LYSO, and PAA Substrates Recrystallized at a Series of Temperatures[a]

Recrystallization Temperature (°C)	Substrates			
	PVA	LYSO	PVPY	PAA
45	F(∥=)[a]	F(∥)	F(∥)	---
30	E(=)[b]	F(∥)	F(∥)	---
15	E(=)	E(=)	F(∥)	---
0	E(=)	E(=)	F(∥)	---
-15	E(=)	E(=)	E(=)	---
-30	E(=)	E(=)	E(=)	---

[a] F(∥) and E(=) represent the flat-on and edge-on lamellar orientations.

temperature and the polymer/substrate interfacial energy. Considering flat-on and edge-on lamellae must develop from the primary nucleus, then flat-on and edge-on primary nucleus on the substrates are shown in Scheme 1. The free energy for flat-on nucleation is

$$\Delta G_F = 4la\sigma_{CM} + a^2(\sigma_{eCM} + \sigma_{eCS} - \sigma_{MS}) - a^2l\Delta f \quad (2)$$

where l and a are the dimensions of the nucleus, σ_{CM}, σ_{eCM}, σ_{eCS}, and σ_{MS} are the interfacial free energy of lateral plane of crystal and melts, folding plane of crystal and melts, folding plane of crystal and substrates, and melts and substrates, respectively. Δf is the free energy change on crystallization per unit volume and

$$\Delta f = \frac{\Delta h \Delta T}{T_m^0} \quad (3)$$

where Δh is the heat of fusion, T_m^0 is the equilibrium melting point, and $\Delta T = T_m^0 - T$ is the degree of supercooling.

The critical size and free energy can be calculated by $\partial\Delta G_F/\partial a = \partial\Delta G_F/\partial l = 0$, and the critical free energy for flat-on nucleation is

$$\Delta G_F^* = \frac{16\sigma_{CM}{}^2(\sigma_{eCM} + \sigma_{eCS} - \sigma_{MS})}{\Delta f^2} \quad (4)$$

The free energy for edge-on nucleation shown in Scheme 1 is

$$\Delta G_E = 2ac\sigma_{eCM} + 2lc\sigma_{CM} + la(\sigma_{CM} + \sigma_{CS} - \sigma_{MS}) - acl\Delta f \quad (5)$$

The critical free energy for edge-on nucleation is

$$\Delta G_E^* = \frac{16\sigma_{eCM}\sigma_{CM}(\sigma_{CM} + \sigma_{CS} - \sigma_{MS})}{\Delta f^2} \quad (6)$$

dx.doi.org/10.1021/ma102973w |*Macromolecules* 2011, 44, 3511–3516

Scheme 1. (a) Flat-On and (b) Edge-On Primary Nucleus on the Substrates

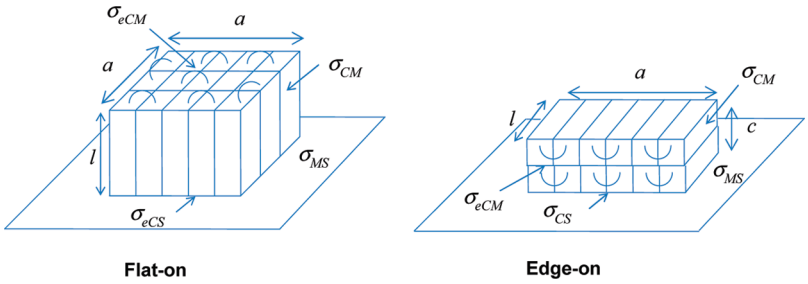

The favorite type of lamellar orientation is determined by the difference of the critical free energy of the primary nucleation (eqs 4 and 6).

$$\Delta G_F^* - \Delta G_E^* = \frac{16\sigma_{CM}[\sigma_{CM}(\sigma_{eCS} - \sigma_{MS}) - \sigma_{eCM}(\sigma_{CS} - \sigma_{MS})]}{\Delta f^2} \quad (7)$$

We relate the interfacial free energy to the surface tension according to Fowkes theory on the interfacial energy, i.e., $\sigma_{ab} = (\sigma_a^{1/2} - \sigma_b^{1/2})^2$, and our final result of the free energy difference between flat-on nucleation and edge-on nucleation is

$$\Delta G_F^* - \Delta G_E^* = \frac{32(\sigma_{eC}^{1/2} - \sigma_C^{1/2})(\sigma_{eC}^{1/2} - \sigma_M^{1/2})}{\Delta f^2} (\sigma_C^{1/2} - \sigma_M^{1/2})^3(\sigma_S^{1/2} - \sigma_M^{1/2}) \quad (8)$$

Thus, we may predict the orientation of lamellae from the deference of surface energies among σ_{eC}, σ_C, σ_M, and σ_S. The folding surface energy σ_{eC} is always larger than the lateral surface energy σ_C and surface energy of polymer melts σ_M at the same temperature; therefore, the orientation of lamellae only depends on $\sigma_C^{1/2} - \sigma_M^{1/2}$ and $\sigma_S^{1/2} - \sigma_M^{1/2}$. In the case of $\sigma_C > \sigma_M$, it can be concluded that the orientation will change from flat-on to edge-on with the increasing of surface free energy of substrates. In the case of $\sigma_M > \sigma_C$, the orientation will change from edge-on to flat-on with the increasing of surface free energy of substrates. Because of the weak dependence of the solid surface energy on temperature, the transition only depends on the surface tension of polymer melts at $\sigma_C = \sigma_M(T^*)$ and at certain temperature T^* and surface energy of substrates σ_S^*. σ_{M0} is the σ_M when the temperature is at T_g. The phase diagram of the lamellar orientation on the substrates with different surface energies is shown in Figure 4. The diagram clearly shows the good agreement between the experimental observation in Table 1 and the theoretical prediction of eq 8. We even may estimate the surface energy of LYSO from our model by using the critical surface energy $\sigma_S^* = \sigma_M(T)$. The surface energy of PEO melts depends on the temperature by Roe[29]

$$\sigma_{PEO} = 42.8 - 0.076(T - 20) \quad (9)$$

On the basis of the experimental results that the transition temperature for LYSO in 15−30 °C and for PVPY in 0−15 °C (Table 1), the transition surface energy from edge-on to flat-on orientation may be estimated as $\sigma_S^* = \sigma_{PEO}(22.5\ °C) = 42.6$ mJ/m^2 for LYSO substrate and $\sigma_S^* = \sigma_{PEO}(7.5\ °C) = 43.8$ mJ/m^2 for PVPY substrate. The results are in good agreement with the experimental measurement of PVPY surface energy (the surface energies of PVA, PVPY, and PEO are 37, 46, and 43 mJ/m^2, respectively[30,31]) Zhu et al.[4] reported the temperature dependence of the lamellar orientation previously, which also confirm the valid of our model that the orientation is determined by the favorite primary nucleus.

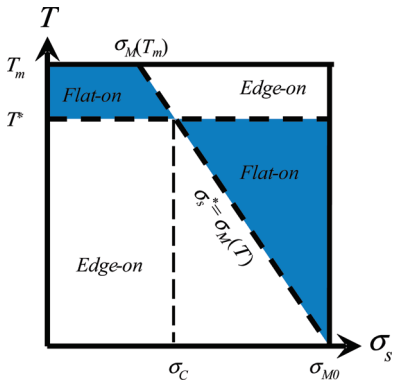

Figure 4. Phase diagram of the lamellar orientation in the thin film.

CONCLUSION

Wetting and dewetting behaviors of PEO melts on different substrates were observed in situ using AFM at 75 °C. The results clearly indicate that wetting of the PEO melt took place on LYSO, PVPY, and PAA substrates, while dewetting of the PEO melt occurred on PVA substrate. The larger the interfacial free energy, the faster the dewetting process (on PVA substrate) takes place, while the smaller the interfacial free energy, the faster the wetting process (on PAA substrate) occurs. Lamellar orientations of recrystallized PEO on the substrates were investigated using AFM and TEM ED pattern. The results show that both the degree of supercooling and PEO/substrate interfacial free energy have a significant influence on the lamellar orientation of the PEO crystals. Both the lower the interfacial free energy and the larger the supercooling degree are needed to induce the transition from flat-on to edge-on lamellae. A thermodynamic model was proposed to predict the dependence of the lamellar orientation on the degree of supercooling and the surface free energy of substrates. Our model suggests that the surface free energy of PEO melt is equal to the surface energy of substrate at the transition point from flat-on to edge-on lamellae. The observed temperature and surface energy dependence of the lamellar orientation in our work supported our model qualitatively.

dx.doi.org/10.1021/ma102973w |*Macromolecules* 2011, 44, 3511–3516

■ ASSOCIATED CONTENT

Supporting Information. AFM height images and the corresponding cross-section analysis of PEO single crystals annealed at 75 °C for a period of time on PVA, LYSO, PVPY, and PAA substrates; AFM images of PEO recrystallized at some special temperatures on different substrates. This material is available free of charge via the Internet at http://pubs.acs.org.

■ AUTHOR INFORMATION

Corresponding Author
*E-mail: lilinll@bnu.edu.cn. Phone: +86-10-62207629.

■ ACKNOWLEDGMENT

This work was supported by the National Science Foundation of China (Grants 20634050, 20804053, 50521302, 50833006, and 20974115) and the National Basic Research Program of China (973 Project Grant 2007CB936400).

■ REFERENCES

(1) Frank, C. W.; Rao, V.; Despotopoulou, M. M.; Pease, R. F.; Hinsberg, W. D.; Miller, R. D.; Rablot, J. F. *Science* **1996**, *273*, 912–915.
(2) Calvert, P. *Nature* **1996**, *384*, 311–312.
(3) Seki, T.; Fukuda, K.; Ichimura, K. *Langmuir* **1999**, *15*, 5098–5101.
(4) Zhu, L.; Cheng, S. Z. D.; Calhoun, B. H.; Ge, Q.; Quirk, R. P.; Thomas, E. L.; Hsiao, B. S.; Yeh, F.; Lotz, B. *J. Am. Chem. Soc.* **2000**, *122*, 5957–5967.
(5) Huang, P.; Zhu, L.; Cheng, S. Z. D.; Ge, Q.; Quirk, R. P.; Thomas, E. L.; Lotz, B.; Hsiao, B. S.; Liu, L. Z.; Yeh, F. J. *Macromolecules* **2001**, *34*, 6649–6657.
(6) Kawashima, K.; Kawano, R.; Miyagi, T.; Umemoto, S.; Okui, N. *J. Macromol. Sci., Part B* **2003**, *42*, 889–899.
(7) Jeon, K.; Krishnamoorti, R. *Macromolecules* **2008**, *41*, 7131–7140.
(8) Wang, Y.; Chan, C. M.; Ng, K. M.; Li, L. *Macromolecules* **2008**, *41*, 2548–2553.
(9) Ma, Y.; Hu, W.; Reiter, G. *Macromolecules* **2006**, *39*, 5159–5164.
(10) Wang, Y.; Ge, S.; Rafailovich, M.; Sokolov, J.; Zou, Y.; Ade, H.; Lüning, J.; Lustiger, A.; Maron, G. *Macromolecules* **2004**, *37*, 3319–3327.
(11) Liang, Y.; Zheng, M.; Park, K. H.; Lee, H. S. *Polymer* **2008**, *49*, 1961–1967.
(12) Hu, Z.; Zhang, F.; Du, B.; Huang, H.; He, T. *Langmuir* **2003**, *19*, 9013–9017.
(13) Schönherr, H.; Frank, C. W. *Macromolecules* **2003**, *36*, 1188–1198.
(14) Mareau, V. H.; Prud'homme, R. E. *Macromolecules* **2005**, *38*, 398–408.
(15) Wang, Y.; Rafailovich, M.; Sokolov, J.; Gersappe, D.; Araki, T.; Zou, Y.; Kilcoyne, A. D. L.; Ade, H.; Marom, G.; Lustiger, A. *Phys. Rev. Lett.* **2006**, *96*, 028303.
(16) Zheng, Y.; Bruening, M. L.; Baker, G. L. *Macromolecules* **2007**, *40*, 8212–8219.
(17) Qiao, C.; Zhao, J.; Jiang, S.; Ji, X.; An, L.; Jiang, B. *J. Polym. Sci., Part B* **2005**, *43*, 1303–1309.
(18) Hu, Z.; Huang, H.; Zhang, F.; Du, B.; He, T. *Langmuir* **2004**, *20*, 3271–3277.
(19) Kikkawa, Y.; Abe, H.; Fujita, M.; Iwata, T.; Inoue, Y.; Doi, Y. *Macromol. Chem. Phys.* **2003**, *204*, 1822–1831.
(20) Liu, Y. X.; Chen, E. Q. *Coord. Chem. Rev.* **2010**, *254*, 1011–1037.
(21) kovacs, A. J.; Gonthier, A.; Kolloid, Z. Z. *Polymer* **1972**, *250*, 530–551.
(22) Balta Calleja, F. J.; Keller, A. *J. Polym. Sci.* **1964**, *A2*, 2171–2179.
(23) Balta Calleja, F. J. Ph. D. Thesis, Bristol University, 1962.
(24) Zhao, W.; Rafailovich, M. H.; Sokolov, J.; Fetters, L. J.; Plano, R.; Sanyal, M. K.; Sinha, S. K.; Sauer, B. B. *Phys. Rev. Lett.* **1993**, *70*, 1453–1456.
(25) Faldi, A.; Composto, R. J.; Winey, K. I. *Langmuir* **1995**, *11*, 4855–4861.
(26) Hsiao, M. S.; Chen, W. Y.; Zheng, J. X.; Van Horn, R. M.; Quirk, R. P.; Ivanov, D. A.; Thomas, E. L.; Lotz, B.; Cheng, S. Z. D. *Macromolecules* **2008**, *41*, 4794–4801.
(27) Khutoryanskiy, V. V.; Dubolazov, A. V.; Nurkeeva, Z. S.; Mun, G. A. *Langmuir* **2004**, 20.
(28) Lutkenhaus, J. L.; Hrabak, K. D.; McEnnis, K.; Hammond, P. T. *J. Am. Chem. Soc.* **2005**, *127*, 17228–17234.
(29) Roe, R. J. *J. Phys. Chem.* **1968**, *72*, 2013–2017.
(30) Wu, S. In *Polymer Interface and Adhesion*, 1st ed.; Marcel Dekker: New York, 1982; pp 185−189.
(31) Wu, S. In *Polymer Handbook*, 3rd ed.; Brandrup, J., Immergut, E. H., Eds.; Wiley: New York, 1989.